CANCER GENOMICS & PROTEOMICS *19*: 591-605 (2022)
doi:10.21873/cgp.20344

Prognostic Significance of the *BIRC2-BIRC3* Gene Signature in Head and Neck Squamous Cell Carcinoma

MIN KYEONG LEE[1], JOO KYUNG NOH[1], SEON RANG WOO[2], MOONKYOO KONG[3], YOUNG CHAN LEE[2], JUNG WOO LEE[4], SEONG-GYU KO[5] and YOUNG-GYU EUN[2]

[1]*Department of Biomedical Science and Technology, Graduate School, Kyung Hee University, Seoul, Republic of Korea;*
[2]*Department of Otolaryngology-Head and Neck Surgery, Kyung Hee University Medical Center, Seoul, Republic of Korea;*
[3]*Department of Radiation Oncology, Kyung Hee University Medical Center, Kyung Hee University School of Medicine, Seoul, Republic of Korea;*
[4]*Department of Oral and Maxillofacial Surgery, School of Dentistry, Kyung Hee University, Seoul, Korea;*
[5]*Department of Preventive Medicine, College of Korean Medicine, Kyung Hee University, Seoul, Republic of Korea*

Abstract. *Background/Aim: Head and neck squamous cell carcinoma (HNSCC) has poor prognosis, with survival rates that have not significantly improved over the past several decades. Therefore, prediction of HNSCC prognosis is of clinical importance. Baculoviral IAP Repeat containing 2 (BIRC2) and Baculoviral IAP Repeat containing 3 (BIRC3) are involved in oncogenic activity by modulating cell proliferation, apoptosis and invasion in HNSCC. This study aimed to develop and validate a predictive gene signature for BIRC2 and BIRC3. Materials and Methods: The genomic copy number and gene expression for BIRC2 and BIRC3 were systematically explored in patients with HNSCC to investigate the clinical relevance of BIRC2 and BIRC3 activation. A prognostic signature was developed based on correlations associated with BIRC2 and BIRC3 mRNA expression and copy number alterations. Hierarchical clustering was used to classify the clusters (Clusters 1 and 2). Moreover, independent validation of the BIRC2-BIRC3 gene signature was performed using the Leipzig, MDACC, FHCRC, and KHU datasets. To explore the biological functions of the BIRC2-BIRC3 gene signature, string analysis and pathway annotation were also performed. Results: BIRC2-BIRC3 gene signature-derived cluster 2 patients exhibited significantly poor survival. This signature also predicted survival in three independent cohorts. Interestingly, the BIRC2-BIRC3 gene signature additionally permitted the identification of survival in advanced tumor stages with excellent accuracy in all three cohorts. Multivariate Cox regression analysis identified that the BIRC2-BIRC3 signature was an independent predictor associated with the survival of patients with HNSCC. Moreover, Inhibition of BIRC2 modulated the NF-κB signaling pathway via upregulation of CBR1 expression. Conclusion: The BIRC2-BIRC3 gene signature was found to be associated with the prognosis of HNSCC. Thus, BIRC2 and BIRC3 could be potential targets for improving HNSCC prognosis.*

Correspondence to: Young-Gyu Eun, MD, Ph.D., Department of Otolaryngology-Head and Neck Surgery, Kyung Hee University Medical Center, Kyungheedaero23, Dongdaemun-gu, Seoul, Republic of Korea. Tel: +82 29588474, Fax: +82 29588470, e-mail: ygeun@khu.ac.kr

Key Words: BIRC2, BIRC3, gene signature, head and neck cancer, prognosis.

Head and neck squamous cell carcinoma (HNSCC) is the sixth most common cancer worldwide, with more than 600,000 patients diagnosed annually (1). There are several risk factors that can increase one's risk of developing HNSCC - including tobacco use, alcohol consumption and poor oral hygiene. In addition, infection with human papillomavirus (HPV) can also cause HNSCC (2, 3). Over the past few years, several preclinical and clinical studies of HNSCC have been dedicated to the development of new treatment techniques for overcoming this cancer (4). Despite these efforts, the 5-year survival rate is reported to be approximately 60% for all HNSCC cases, with an annual death toll of 380,000 (5). Moreover, patients exhibit a highly heterogeneous treatment response. Therefore, the establishment of individual tumor biology through appropriate gene signatures must be taken

Table I. *Clinical and pathological features of HNSCC in 5 cohorts.*

	TCGA cohort	Leipzig cohort	MDACC cohort	FHCRC cohort	KHU cohort
Number of patients	520	270	74	97	75
Sex					
Male	384 (73.8%)	223 (82.6%)	58 (78.4%)	66 (68.0%)	58 (77.3%)
Female	136 (26.2%)	47 (17.4%)	16 (21.6%)	31 (32.0%)	17 (22.6%)
Age (mean±SD)	62.2±15.3	60.1±10.0	58.1±13.6	NA	63.5±11.8
Anatomic site					
Oral cavity	315 (60.5%)	83 (30.7%)	71 (95.9%)	86 (88.7%)	49 (67.1%)
Oropharynx	79 (15.1%)	102 (37.8%)	3 (4.1%)	11 (11.3%)	11 (15.1%)
Larynx	116 (22.3%)	48 (17.8%)	0	0	9 (12.3%)
Hypopharynx	10 (1.9%)	33 (12.2%)	0	0	4 (5.5%)
Others		4 (1.5%)	0	0	0
Primary tumor					
T1	35 (6.8%)	35 (13.0%)	3 (4.1%)	NA	21 (28%)
T2	151 (29.4%)	80 (29.6%)	27 (36.5%)	NA	15 (20%)
T3	132 (25.8%)	58 (21.5%)	28 (37.8%)	NA	5 (6.6%)
T4	195 (38.0%)	97 (35.9%)	16 (21.6%)	NA	28 (37.3%)
Regional lymph node					
N0	244 (48.1%)	94 (34.8%)	NA	NA	37 (49.3%)
N1	83 (16.4%)	32 (11.9%)	NA	NA	10 (13.3%)
N2	162 (32.0%)	132 (48.9%)	NA	NA	19 (25.3%)
N3	18 (3.5%)	12 (4.4%)	NA	NA	1 (1.3%)
Stage					
I	20 (4.0%)	18 (6.7%)	3 (4.1%)	30 (30.9%)	16 (21.3%)
II	98 (19.3%)	37 (13.7%)	16 (21.6%)	22 (11.3%)	17 (22.6%)
III	105 (20.7%)	37 (13.7%)	15 (20.3%)	26 (15.5%)	6 (8%)
IV	283 (56.0%)	178 (65.9%)	40 (54.1%)	52 (42.3%)	26 (34.6%)
HPV status					
Positive	68 (19.9%)	60 (23.4%)	NA	0	4 (5.3%)
Negative	274 (80.1%)	196 (76.6%)	NA	97 (100%)	16 (21.3%)
Tobacco use					
Never	114 (23.3%)	48 (17.8%)	15 (20.3%)	NA	25 (33.3%)
Yes	376 (76.7%)	222 (82.2%)	59 (79.7%)	NA	50 (66.6%)
Alcohol use					
Never	162 (31.8%)	31 (11.5%)	NA	NA	NA
Yes	347 (68.2%)	239 (88.5%)	NA	NA	NA
BIRC2-BIRC3 gene signature					
Cluster 1	189 (36.3%)	122 (45.1%)	27 (36.4%)	46 (47.4%)	36 (48%)
Cluster 2	331 (63.7%)	148 (54.8%)	41 (55.4%)	51 (52.5%)	39 (52%)

into consideration for estimating treatment response and improving patient survival.

The Baculoviral IAP Repeat containing 2 (BIRC2) and Baculoviral IAP Repeat containing 3 (BIRC3) genes are members of the inhibitor of apoptosis (IAP) family, which plays a role in the regulation of the caspase pathway to prevent apoptosis. BIRC2 and BIRC3 are mainly involved in the programmed cell death pathway, which promotes cell survival, cellular differentiation, cell division, signal transduction and cell response to damage. In cancer cells, BIRC2 and BIRC3 are linked to their overexpression, which is associated with drug resistance and poor prognosis (6). In addition, copy number amplification of the 11q22.1-q22.2 regions, encoding BIRC2 and BIRC3, has been frequently identified in several cancers (7, 8) and is associated with lymph node metastasis as well as poor clinical outcomes (9).

The present study systematically analyzed BIRC2 and BIRC3 related genomic data of patients with HNSCC from multiple cohorts and developed a BIRC2-BIRC3 gene signature. We also identified the biological mechanisms associated with this signature.

Materials and Methods

Study design and gene expression data. Genomic data from TCGA, including RNA-seq (Illumina HiSeq) data of gene expression, gene-level copy number alterations (CNAs) and clinical data (TCGA cohort, *n*=566), were obtained using the UCSC Xena browser

Table II. *Primer sequences for RT-PCR.*

Gene	Forward primer sequence (5'-3')	Reverse primer sequence (3'-5')
BIRC2	ATTGGATTCGGAAGCCCCAA	GAACGCCGAGGGCTAAGTTT
BIRC3	ACTTAGTCTAATCTCGGGAGGTA	ATGTGCCAGTAGGAGACTGC
CBR1	CAGAGACCCCTGTGTACTTG	CAACTCAGGACAAGG TACAAAATG3
P65	GCACCCTGACCTTGCCTATT	CTGCTTGGCGGATTAGCTCT
β-actin	CACCATTGGCAATGAGCGGTTC	AGGTCTTTGCGGATGTCCACGT

(https://xenabrowser.net/). The validation dataset included three independent GEO datasets: the Leipzig cohort (GSE65858, *n*=270), FHCRC cohort (GSE41613, *n*=97) and MDACC cohort (GSE42743, *n*=74), which were downloaded from the National Center for Biotechnology Information Gene Expression Omnibus database (http://www.ncbi.nlm.nih.gov/geo). The KHU cohort was obtained from the Department of Otolaryngology-Head and Neck Surgery, School of Medicine, Kyung Hee University (IRB: 2018-05-046). The cancer cell line encyclopedia data were acquired from CCLE (https://portals.broadinstitute.org/ccle). The clinical characteristics of the patients in the five cohorts are summarized in Table I.

RNA preparation and NGS sequencing. RNA samples were extracted using TRIzol (Invitrogen, Carlsbad, CA, USA). To ensure the quality of the samples for sequencing, Nanodrop (IMPLEN, CA, USA) and Qubit 2.0 (Life Technologies, CA, USA) were used to determine the purity, concentration and integrity of the RNA samples. RNA was extracted and quantified according to the manufacturer's instructions.

RNA sequencing, preprocessing, and transcriptome analysis were performed using Macrogen Inc. (Seoul, Korea). Total RNA concentration was calculated by Quant-IT RiboGreen (Invitrogen, #R11490). Only high-quality RNA preparations with RNA integrity number (RIN) greater than 7.0 were used for RNA library construction. A sequencing library was generated using 1 μg of total RNA from each sample using an Illumina TruSeq Stranded mRNA Sample Prep Kit (Illumina, Inc., San Diego, CA, USA, #RS-122-2101).

Construction and validation of BIRC2-BIRC3 gene signature. The gene expression data set TCGA (*n*=566) was downloaded to construct BIRC2 and BIRC3 associated gene signatures (named BIRC2-BIRC3 gene signature). Seventy-three gene lists (BIRC2- or BIRC3-related genes) were established using a double-correlation approach. First, BIRC2-related genes were identified. BIRC2 copy number-associated genes were determined by analyzing the Pearson correlation between the copy number of BIRC2 and the mRNA expression of each gene (121 genes). BIRC2 mRNA-associated genes were identified by analyzing the Pearson correlation between the mRNA expression of BIRC2 and mRNA expression of each gene (1767 genes). The 55 genes were filtered using a correlation coefficient (greater than 0.25 or less than –0.25) and a *p*-value (less than 0.01). Thereafter, BIRC3-related genes were established as well. BIRC3 copy number-associated genes were identified by analyzing the Pearson correlation between the copy number of BIRC3 and the mRNA expression of each gene (121 genes). Similarly, BIRC3 mRNA-associated genes were identified by analyzing the Pearson correlation between mRNA expression of BIRC3 and mRNA expression of each gene (genes). The 25 genes were filtered according to the correlation coefficient (greater than 0.25 or less than –0.25) and *p*-value (less than 0.01). Seven genes overlapped with BIRC2- and BIRC3-related genes. Furthermore, hierarchical clustering analysis was performed based on the centered average method (10), followed by clustering analysis performed using a cluster 3.0 program. (Stanford University, Stanford, CA, USA). The Bayesian compound covariate algorithm method (BCCP) was used to classify clusters in each patient from the validation sets. Gene expression data of TCGA was adapted to BCCP algorithm to classify clusters, and and then these were estimated according to the misclassification rate determined during leave-one-out cross-validation of the training set using BRB–ArrayTools (https://brb.nci.nih.gov/BRB-ArrayTools/) (11).

Functional annotation and pathway analysis. To explore the biological function of the BIRC2-BIRC3 gene signature, string analysis (using the STRING online tool at https://string-db.org/) and pathway annotation were performed. Combination scores >0.9, degrees >10 and MCODE scores >10 were selected. The pathway was determined by Kyoto Encyclopedia of Genes and Genomes (KEGG) analysis and was considered to be significant with an FDR<0.05.

Cell lines. The HNSCC cell line, SNU1041, was obtained from Prof. Chul Ho Kim (Ajou University). SCC4 and HSC3 were purchased from the American Type Culture Collection (ATCC) and the Japanese Cancer Resources Bank (JCRB), respectively. HSC3 and SNU1041 cells were cultured in RPMI-1640 (Corning, Manassas, VA, USA) and SCC4 cells were cultured in Dulbecco's modified Eagle's medium (DMEM)/F12 (Corning). The media was supplemented with 10% FBS and 1% penicillin-streptomycin (Corning). All the cell lines were cultured at 37˚C in an atmosphere of 5% CO_2.

Reagents. Antibodies were purchased from their respective sources, as follows: BIRC2 and BIRC3 from Santa Cruz Biotechnology (sc-271419, sc-517317, Santa Cruz, CA, USA), CBR1 from Novus (NBP1-86595, Colorado Centennial, CA, USA), P65 from Cell Signaling Technology (8242S , Beverly, MA, USA), as well as β-actin from Santa Cruz Biotechnology (sc-47778, Santa Cruz, CA, USA). The plasmid transfection agent, RNAiMAX, was obtained from Thermo Fisher Scientific (Waltham, MA, USA).

Plasmid transfection. The GFP-conjugated vector or BIRC2 plasmid (hs.Ri.BIRC2.13.1) was transfected into a 6-well plate dish that was filled to a concentration of up to 70% confluency. The GFP-conjugated (pCMV6-AC-GFP) empty vector was purchased from Bioneer (Daejeon, Korea). The siRNA was purchased from IDT (Cambridge, MA, USA). All cells were transfected with siRNA

Table III. *Gene associated with BIRC2*.

TCGA RNA sequencing gene symbol	Correlation coefficient with copy number of BIRC2	*p*-Value of correlation with copy number of BIRC2	Correlation coefficient with gene expression of BIRC2	*p*-Value of correlation with gene expression of BIRC2
ALPP	0.30	2.72E-12	0.30	3.11E-12
AMOTL1	0.26	2.22E-09	0.29	1.1E-11
ARHGAP42	0.35	7.6E-16	0.45	7.6E-27
BIRC2	0.84	4E-135	1.00	3.56E-07
BIRC3	0.28	9.12E-11	0.47	3.46E-29
C11orf70	0.42	1.61E-23	0.45	5.55E-27
CCDC90B	0.27	4.3E-10	0.28	5.92E-11
CHORDC1	0.26	1.24E-09	0.28	6.98E-11
CSMD3	0.26	2.15E-09	0.26	1.35E-09
CWC15	0.31	4.1E-13	0.26	1.12E-09
DCUN1D5	0.63	1.31E-57	0.53	3.92E-38
DYNC2H1	0.37	8.05E-18	0.40	6.55E-21
FADS3	0.26	2.69E-09	0.28	1.43E-10
FCHSD2	0.25	9.29E-09	0.33	2.89E-14
FGF5	0.25	9.33E-09	0.31	8.73E-13
FLJ44054	0.25	6.83E-09	0.29	1.9E-11
FOLR3	0.32	1.82E-13	0.27	8.54E-10
FSTL3	0.32	2.26E-13	0.30	2.08E-12
GLP2R	0.27	8.96E-10	0.30	1.97E-12
KIAA1377	0.45	1.25E-26	0.50	4.17E-34
KRTAP2-1	0.32	1.33E-13	0.25	6.75E-09
L1CAM	0.27	3.56E-10	0.30	6.68E-12
LETM2	0.33	2.43E-14	0.31	4.75E-13
LRRN4	0.32	2.4E-13	0.31	5.18E-13
MED17	0.31	3.09E-13	0.43	5.75E-24
MMP10	0.26	2.27E-09	0.30	5.13E-12
MT1L	0.25	4.9E-09	0.27	3.37E-10
MTMR2	0.33	3.22E-14	0.40	1.67E-21
MYL7	0.30	2.36E-12	0.26	4.51E-09
OR2T1	0.28	8.34E-11	0.28	1.01E-10
PANX1	0.32	1.63E-13	0.40	8.85E-21
PDZD7	0.27	5.97E-10	0.25	5.78E-09
PICALM	0.30	1.86E-12	0.38	3.63E-19
PPFIBP2	–0.27	3.25E-10	–0.28	1.94E-10
PRDM15	–0.26	4.26E-09	–0.25	6.92E-09
PRSS23	0.30	8.69E-12	0.34	1.62E-15
PSG1	0.30	5.67E-12	0.34	2.01E-15
PSG11	0.27	4.93E-10	0.28	7.53E-11
PSG2	0.27	2.62E-10	0.36	5.29E-17
PSG3	0.26	1.98E-09	0.31	1.5E-12
PSG6	0.26	1.72E-09	0.32	2.75E-13
RAB38	0.27	5.93E-10	0.25	5.17E-09
RAB6A	0.27	8.18E-10	0.27	6.59E-10
RAPGEF3	0.29	1.16E-11	0.28	2.01E-10
RELT	0.29	1.27E-11	0.28	2.27E-10
RRAS2	0.29	1.3E-11	0.32	7.86E-14
SERPINH1	0.27	3.65E-10	0.28	1.76E-10
SFTA1P	0.41	4.16E-22	0.38	5.57E-19
SNORA8	0.31	1.15E-12	0.32	4.87E-14
SYT16	0.27	3.48E-10	0.30	4.6E-12
TAF1D	0.41	2.57E-22	0.36	1.55E-17
TMEM123	0.70	1.73E-76	0.77	3.6E-102
TMEM126B	0.31	6.61E-13	0.33	2.47E-14
TMEM133	0.32	9.24E-14	0.42	5.59E-23
YAP1	0.78	1.8E-106	0.83	1.1E-133

using Lipofectamine RNAiMAX Reagent (Life Technologies, Carlsbad, CA, USA), according to the manufacturer's protocol.

Western blot. HNSCC cells were irradiated and lysed using radioimmunoprecipitation assay (RIPA) buffer (50 mM Tris-HCl, 150 mM NaCl, 2 mM EDTA and 1% Triton X-100) containing protease (Roche, Germany) and phosphatase inhibitors (Sigma, USA). Proteins were separated on an SDS-PAGE gel and transferred onto a polyvinylidene difluoride membrane (Millipore, Billerica, MA, USA). The membrane was blocked with 10% skim milk in TBS containing 0.1% Tween-20 (TBS-T) and subsequently incubated with 1: 1000 diluted primary antibody at 4˚C. The horseradish peroxidase-conjugated secondary antibody was diluted to 1:3000 for 2 h at room temperature, and the targeted proteins were detected using an enhanced chemiluminescence detection kit (GE Healthcare, Buckinghamshire, UK), according to the manufacturer's instructions.

Real-time quantitative reverse transcription PCR. Total RNA was isolated using the TRIzol reagent. RNA was extracted using an RNeasy Mini Kit (GeneAll Biotechnology, Seoul, Korea), according to the manufacturer's protocol. Reverse transcription was performed using the qPCRBIO cDNA Synthesis Kit (PCR Biosystems. London, UK) to obtain cDNA. Primer sequences used have been described in Table II. Relative quantities of mRNA were measured using real-time quantitative RT-PCR with TB Green Premix Ex Taq II (Takara). They were calculated following the threshold cycle number, using the expression of β-actin as an endogenous control. Relative mRNA expression levels were measured using the $2^{-\Delta C^t}$ method. All experiments were performed in triplicate, and the values were averaged.

Statistical analysis. Statistical analyses were performed using R (version 3.6.1). The BRB-ArrayTools software program (http://brb.nci.nih.gov/BRB-ArrayTools/) was used to analyze gene expression data. Kaplan-Meier analysis and log-rank test were performed to estimate the prognostic significance of the BIRC2-BIRC3 gene signature in several cohorts between the Cluster 1 and Cluster 2 groups. Univariate and multivariate Cox proportional hazards regression analyses were used to evaluate the hazard ratio between BIRC2 and BIRC3 signatures and clinical pathologic features with OS. Statistical significance was set at $p<0.05$.

Results

Identification of BIRC2-BIRC3 gene signature associated with the prognosis of HNSCC. The copy number alteration of the BIRC2 and BIRC3 genes was analyzed using the cBioPortal database. BIRC2 was amplified in 7% of HNSCC cases and was located in the second highest status among the 32 cancers. (Figure 1A). It was observed that BIRC3 was amplified in HNSCC cells. The copy number of BIRC3 was altered by approximately 7% in HNSCC, which is the second most common status among several cancers (Figure 1B). In addition, there was a positive correlation between mRNA and amplification of BIRC2 (correlation coefficient=0.83, p=2.50e-126; Figure 1C). However, copy number alteration was not the only factor that activated BIRC2 and BIRC3s. As depicted in Figure 1D, there were many samples that highly expressed mRNA without amplification of BIRC2 (in circle). In addition, BIRC3 was the most relevant to BIRC2, and both genes were located on chromosome 11q.22. Therefore, the mRNA expression levels of BIRC2 and BIRC3 were strongly correlated (correlation coefficient=0.46, p=3.47e-27); (Figure 1D). The BIRC2-BIRC3 gene signature was established by identifying associated genes that were significantly related to the mRNA level and copy number alteration of BIRC2 and BIRC3 genes in the TCGA cohort (Figure 2A). The list of 73 genes is provided in Table III and Table IV. According to the unsupervised clustering method, hierarchical clustering analysis was performed to classify the TCGA cohort into two subgroups (Cluster 1 and Cluster 2; Figure 2B). Kaplan-Meier survival curves with log-rank analysis revealed that the two subgroups had different survival profiles, with Cluster 2 having a worse prognosis than Cluster 1 (5-year survival rate: 45.66% *vs*. 50.06%, p=0.003) (Figure 2C).

Validation of the BIRC2-BIRC3 gene signature in four independent cohorts. To validate the prognostic BIRC2-BIRC3 gene signature, the Leipzig, FHCRC, MDACC and KHU cohorts were used as the test data set. The validation process has been illustrated in Figure 2D. The BIRC2-BIRC3 gene signature was applied to four independent cohorts, and prediction was performed using the BCCP algorithm. The BCCP cutoff value was selected using a receiver operating characteristic (ROC) curve. The closest to the point of maximal sensitivity and specificity was selected as the cut-off value. The BIRC2-BIRC3 signature classified HNSCC patients into Clusters 1 and 2. As expected, Kaplan-Meier analysis revealed that cluster 2 had significantly worse OS than cluster 1 among independent validation datasets: the Leipzig cohort (38.70% OS in Cluster 2 *vs*. in 63.71% Cluster 1 at 5 years, p=0.009 ; Figure 2E), FHCRC cohort (38.46% OS in Cluster 2 *vs*. 66.43% in Cluster 1 at 5 years, p=0.008; Figure 2E), and MDACC cohort (35.4% OS in Cluster 2 *vs*. 64.0% in Cluster 1 at 5 years, p=0.02; Figure 2E). Although the KHU cohort did not have any statistical significance, Cluster 2 had worse recurrence-free survival (RFS) than Cluster 1, as predicted by other cohorts. Their prognostic value exhibited a 71.50% recur free survival rate in Cluster 2 and an 89.88% recur free survival rate in Cluster 1 at 5 years. (p=0.1; Figure 2E). These results highlight the robustness of our BIRC2-BIRC3 gene signature in predicting prognosis in patients with HNSCC.

The BIRC2-BIRC3 gene signature serves as an independent predictor of clinicopathological variables in patients with HNSCC. To further evaluate the performance of our BIRC2-BIRC3 gene signature in various clinicopathological variables, univariate and multivariate Cox hazard regression analyses were performed. Three cohorts (TCGA, Leipzig, and

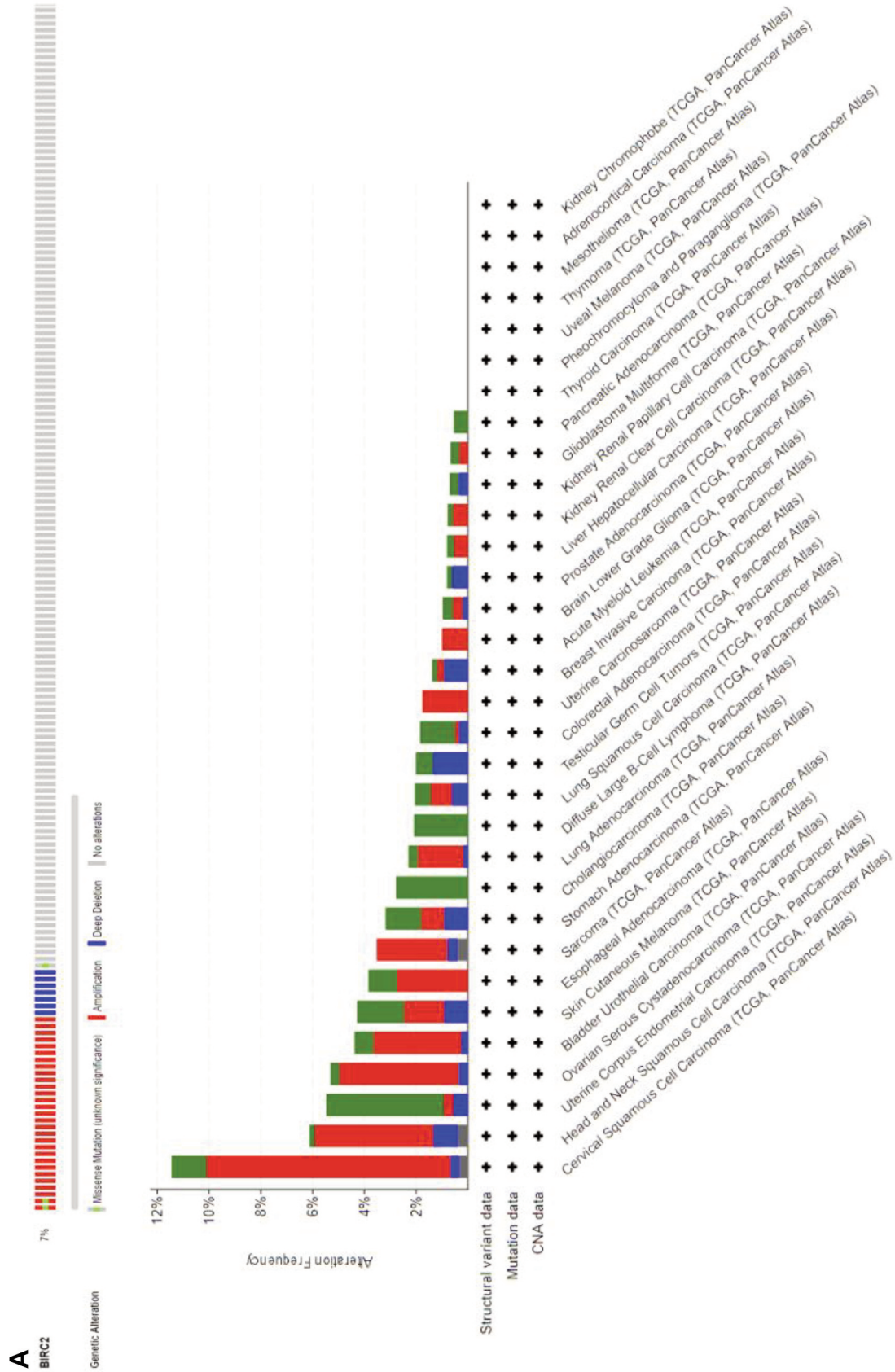

Figure 1. *Continued*

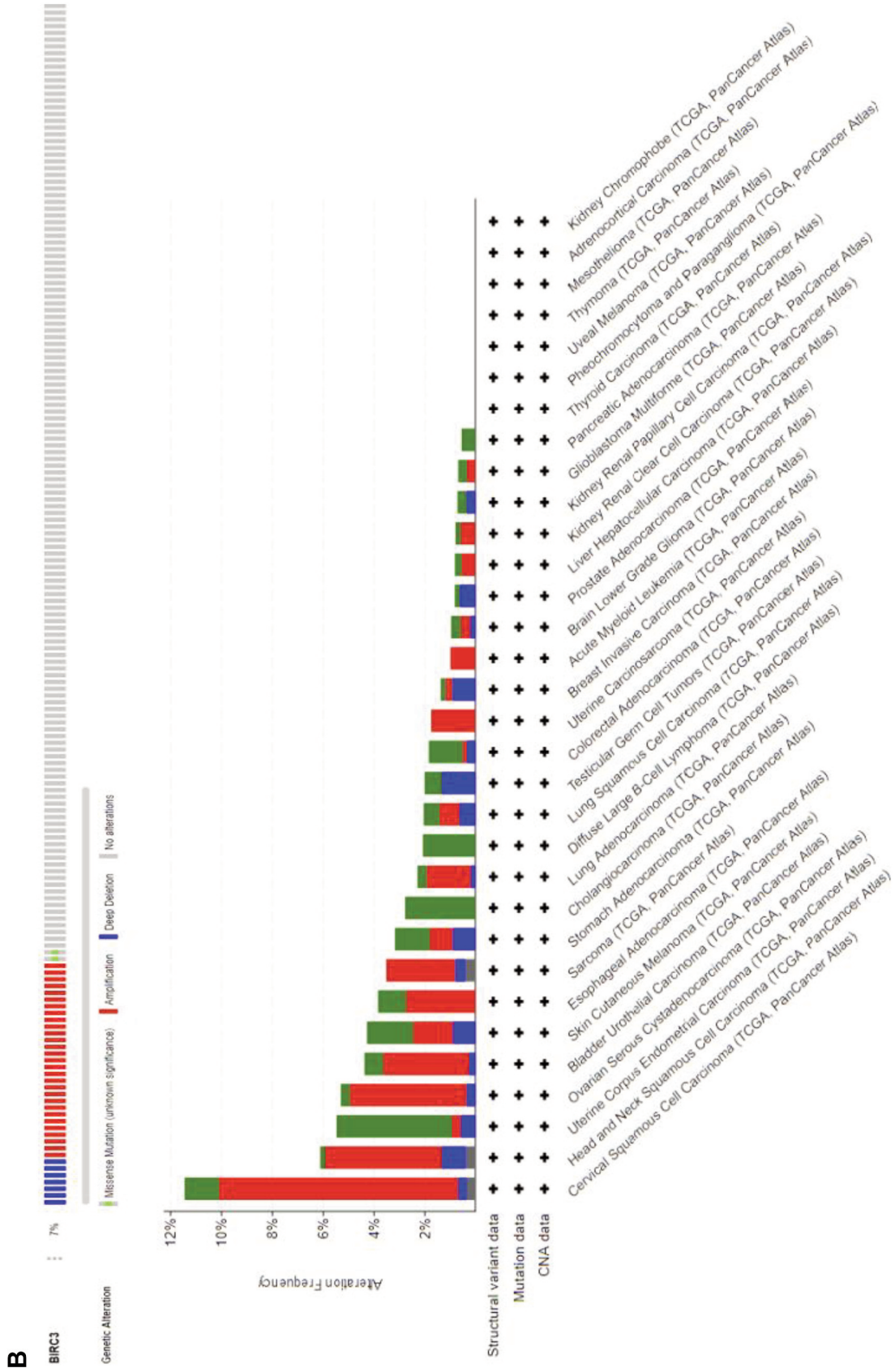

Figure 1. *Continued*

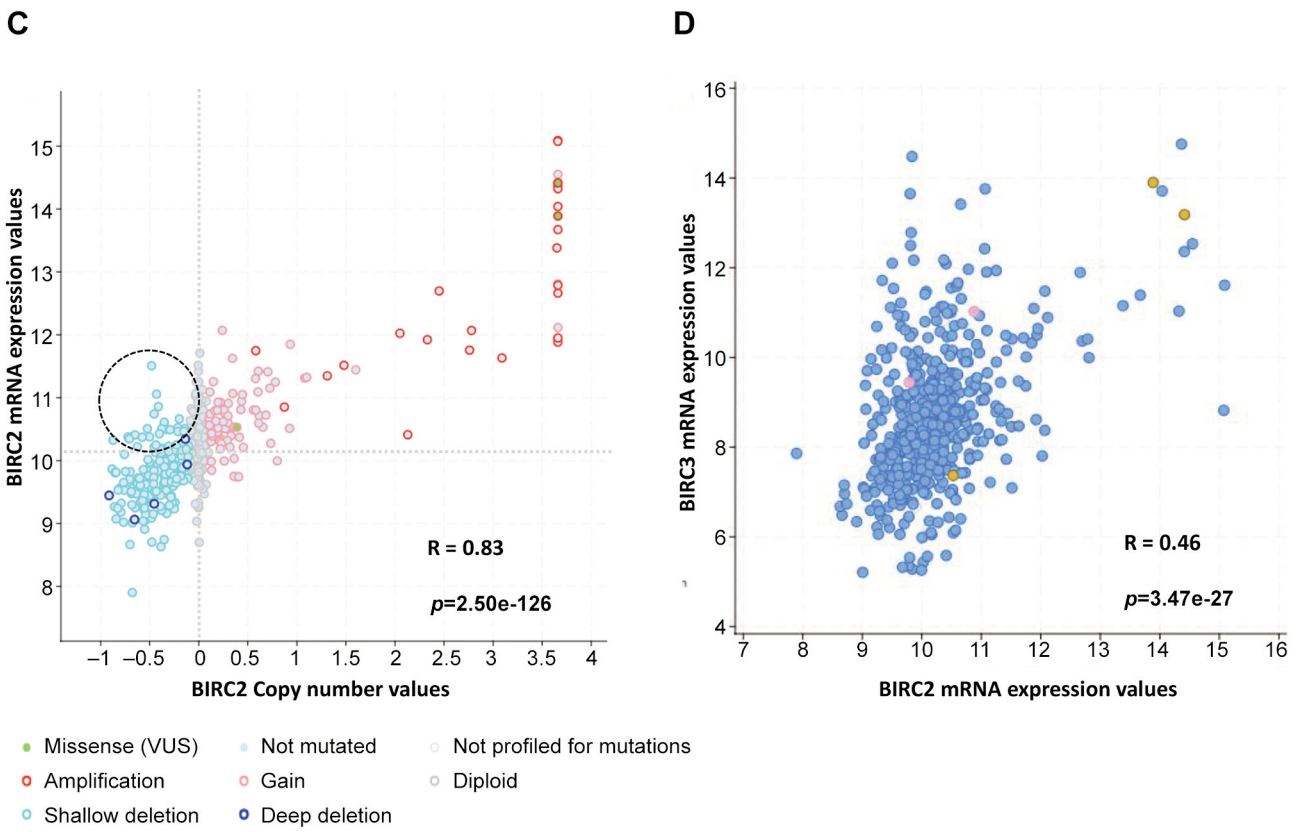

Figure 1. *The alteration of BIRC2 and BIRC3 in HNSCC. (A) Cross-cancer alteration summary for BIRC2 in 32 cancers using genome copy number data from the TCGA Cohorts. HNSCC was located in the second highest amplified cancer type (7%). (B) Cross-cancer alteration summary for BIRC3 in 32 cancers genome copy number data from the TCGA cohorts, HNSCC was located in the second-highest amplified cancer type (7%). (C) Activation of BIRC2 without amplification in HNSCC, scatter plots of BIRC2 mRNA expression and copy number alteration in HNSCC patients in the TCGA cohort. (D) The positive correlation of mRNA expression of BIRC2 and BIRC3 genes.*

KHU) contained OS data available for analysis using a Cox proportional hazards model (n=905). Independent clinicopathological variables included patient age, sex, smoking status, alcohol consumption, HPV status, anatomic site, lymph node (LN) metastasis, and T stage. In the univariate analysis, age (<60 years *vs.* ≥60 years), anatomic site (oropharynx *vs.* other sites), HPV status (HPV-positive *vs.* HPV-negative), T stage (T1 and T2 *vs.* T3 and T4), lymph node (LN) metastasis (LN+ *vs.* LN–), as well as BIRC2-BIRC3 gene signature (Cluster 2 *vs.* Cluster 1) emerged as significant predictors of OS (Table V). Multivariate analysis using clinicopathological variables that were statistically significant in the univariate model revealed that T stage, lymph node (LN) metastasis, and BIRC2-BIRC3 gene signature were independent risk factors for predicting OS in HNSCC patients (Table V).

Association of BIRC2-BIRC3 gene signature in specific tumor stages. To further examine the predictability of the BIRC2-BIRC3 gene signature according to tumor stage, HNSCC patients were divided into early stage (stage II, n=116) and advanced stage (stage III.IV, n=384). When BIRC2-BIRC3 gene signature was applied to the early stage, there was no statistically significant difference in survival between the two clusters (p=0.08; Figure 3A). However, patients stratified as Cluster 2 in the advanced stage were significantly associated with a poor prognosis in TCGA (p=4.65e–6; Figure 3B). Similar results were observed in the other two cohorts (Leipzig and FHCRC). In the Leipzig cohort, the BIRC2-BIRC3 gene signature predicted prognosis in the advanced stage. Kaplan-Meier plots and log-rank tests exhibited significant differences in prognostic OS. Patients in cluster 2 had significantly poorer OS than those in Cluster 1 (n=215, Figure 3D; p=0.02). There was no significant difference in OS between the two clusters in the early stages (n=55, Figure 3C; p=0.7). However, when patients with advanced stage disease in the FHCRC cohort were stratified by the BIRC2-BIRC3 gene signature, Kaplan-

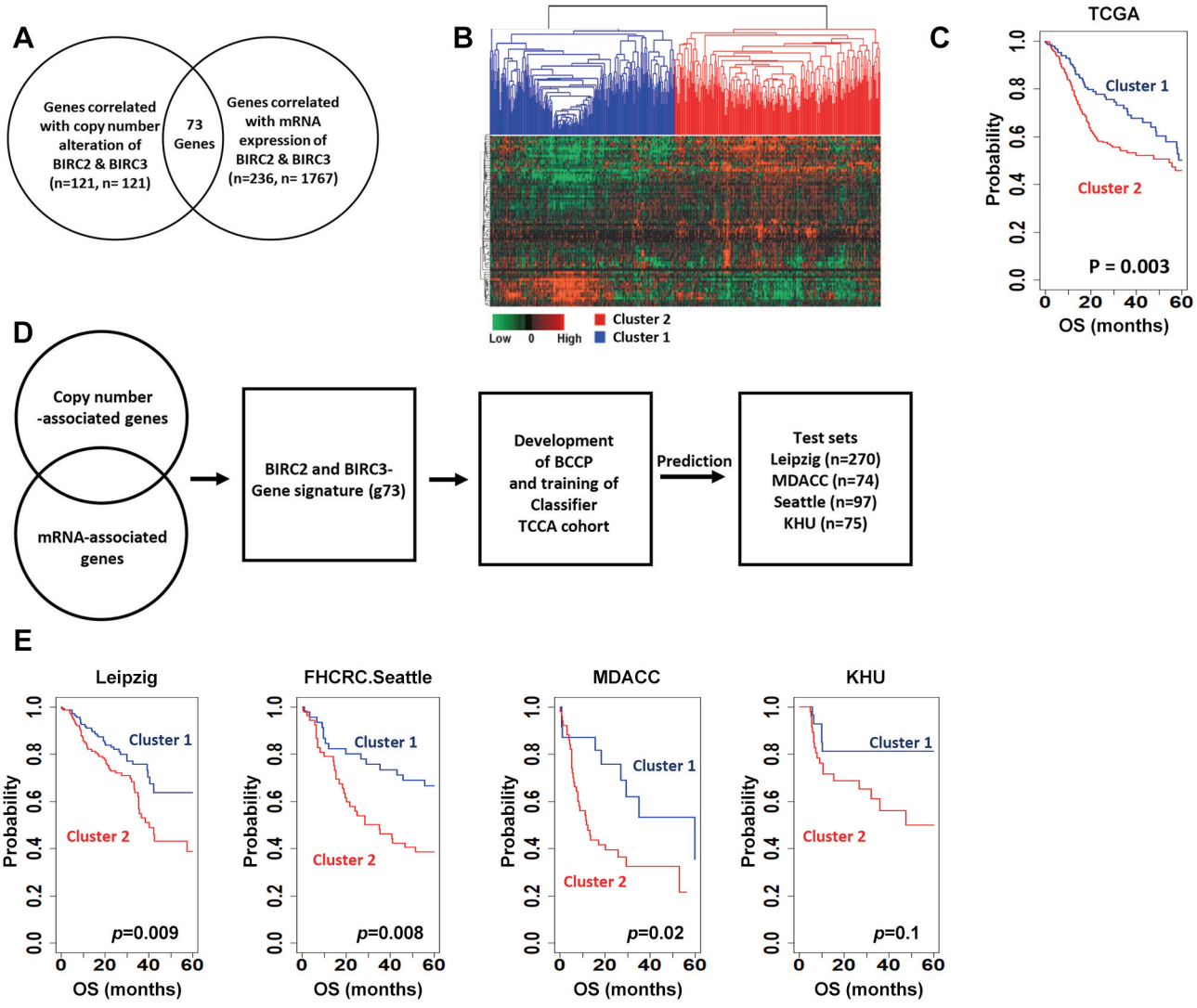

Figure 2. *Development of the Prognostic BIRC2-BIRC3 Gene Signature. (A) Venn diagram of 73 genes that were extracted using a double correlation method. (B) Expression patterns of BIRC2-BIRC3 related gene signature. Classification of Cluster 1 and Cluster 2 by performing centered average method of Hierarchical clustering. (C) Kaplan-Meier plots of overall survival (OS) by BIRC2-BIRC3 gene signature in the TCGA cohort. Patients in Cluster 2 had poorer prognosis than those in Cluster 1 (p=0.003). The p-values were computed by the log-rank test. (D) Schematic flow chart of experimental design and analytic approaches. (E) Kaplan-Meier plots depicting the survival differences overall survival (OS), recur free survival (RFS) between patients in Cluster 1 and Cluster 2 in the Leipzig (p=0.009), FHCRC Seattle (p=0.008), MDACC (p=0.02) and KHU cohorts (p=0.1). The p-values were computed by the log-rank test.*

Meier plots showed significant differences in OS between the two clusters. Cluster 2 showed a significantly worse prognosis than Cluster 1 (n=56, Figure 3F; p=0.009). In contrast, patients in the early stage did not show a significant difference in OS (n=41, p=0.2; Figure 3E). It was thus elucidated that the BIRC2-BIRC3 gene signature, in combination with advanced stages, could predict OS in HNSCC patients. These results suggest that the BIRC2-BIRC3 gene signature might have a potential advantage in predicting prognosis in patients with advanced-stage disease.

KEGG signaling pathway analysis of BIRC2-BIRC3 gene signature. To identify the pathway most closely related to the BIRC2-BIRC3 gene signature, string analysis was performed, and the associated pathway was determined using the Kyoto Encyclopedia of Genes and Genomes (KEGG). Consequently, five significant KEGG pathways were identified in the STRING network. KEGG signaling pathway results were ranked in ascending order according to the size of -log10 (FDR). The NF-κB signaling pathway (FDR=0.01), apoptosis (multiple species, FDR=0.01), apoptosis (FDR=0.03), platinum

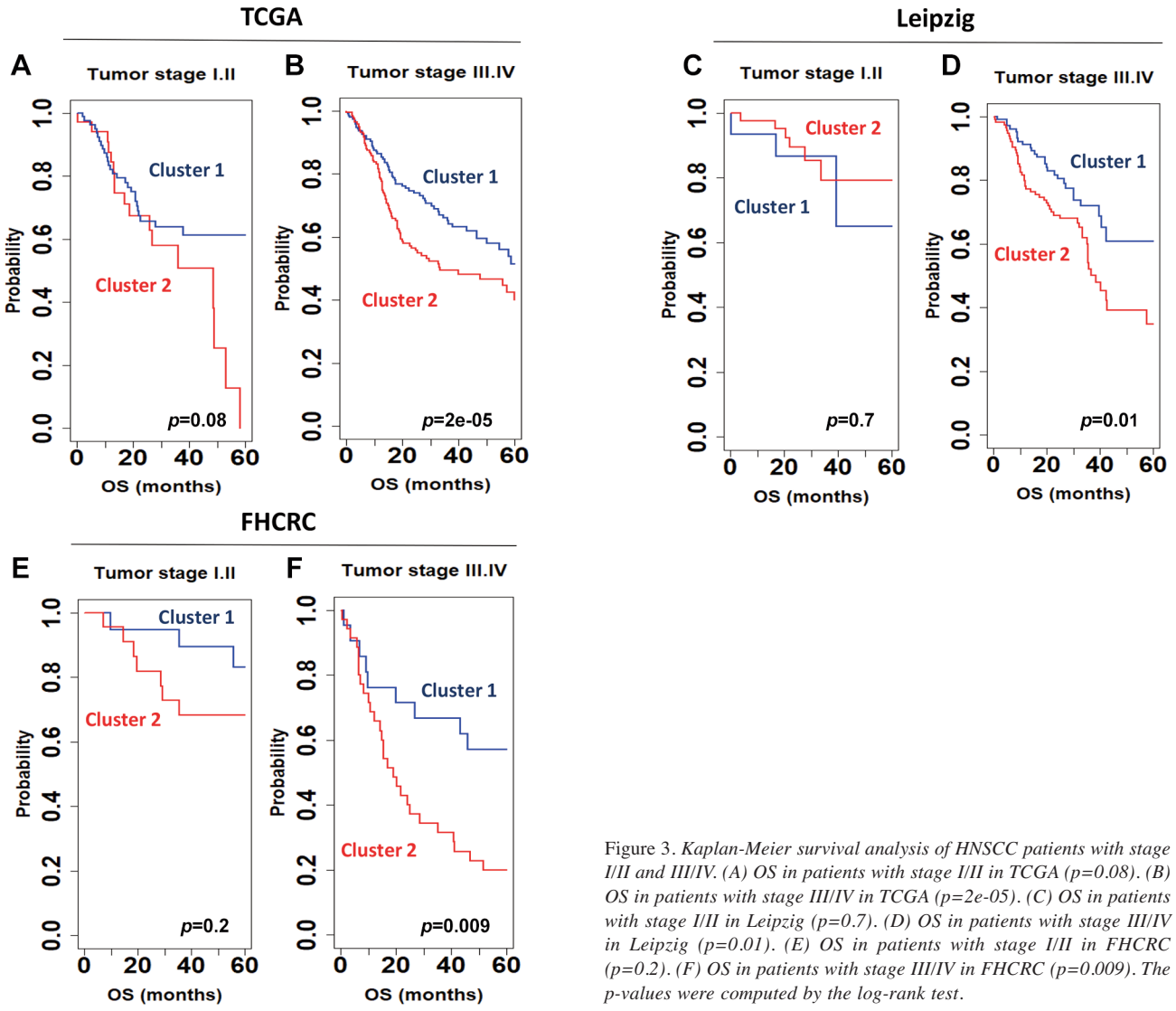

Figure 3. *Kaplan-Meier survival analysis of HNSCC patients with stage I/II and III/IV. (A) OS in patients with stage I/II in TCGA (p=0.08). (B) OS in patients with stage III/IV in TCGA (p=2e-05). (C) OS in patients with stage I/II in Leipzig (p=0.7). (D) OS in patients with stage III/IV in Leipzig (p=0.01). (E) OS in patients with stage I/II in FHCRC (p=0.2). (F) OS in patients with stage III/IV in FHCRC (p=0.009). The p-values were computed by the log-rank test.*

drug resistance (FDR=0.04), and NOD-like receptor signaling pathway (FDR=0.05) are depicted in Figure 4A. The NF-κB signaling pathway was the most relevant among several pathways.

Knockdown of BIRC2 regulates NF-kB signaling pathway by modulating the downstream genes CIAP2 and CBR1. The association of the BIRC2-BIRC3 gene signature with the nuclear factor kappa B (NF-kB) signaling pathway prompted further investigations to identify novel downstream genes regulating the NF-κB signaling pathway. To this end, it was postulated that BIRC2 contributes to the NF-κB signaling pathway *via* CBR1 expression. SNU1041, SCC4, and HSC3 cell lines were selected as the Cluster 2 subgroup in the CCLE cell line data using a BCCP algorithm with the BIRC2-BIRC3 gene signature (Figure 4B). BIRC2 was silenced in three cell lines using siRNA. Inhibition of BIRC2 elevated the mRNA as well as protein expression levels of CBR1, while those of CIAP1 (known as BIRC2), CIAP2 (known as BIRC3), and P65 were decreased (Figure 4C, D). These results suggest that BIRC2 could be a regulator of CIAP2, CBR1 and P65. Subsequently, this study attempted to elucidate the mechanisms of CBR1 and P65. Co-inhibition of BIRC2 and CBR1 was performed using siRNAs. Co-inhibition of target genes decreased CBR1 mRNA and protein expression levels, compared to inhibition of BIRC2. Moreover, P65 mRNA and protein expression levels were recovered compared with BIRC2-targeted siRNA, which was equal to the level obtained by transfection using siGFP (Figure 4E, F), suggesting that BIRC2 regulates P65 expression through CBR1.

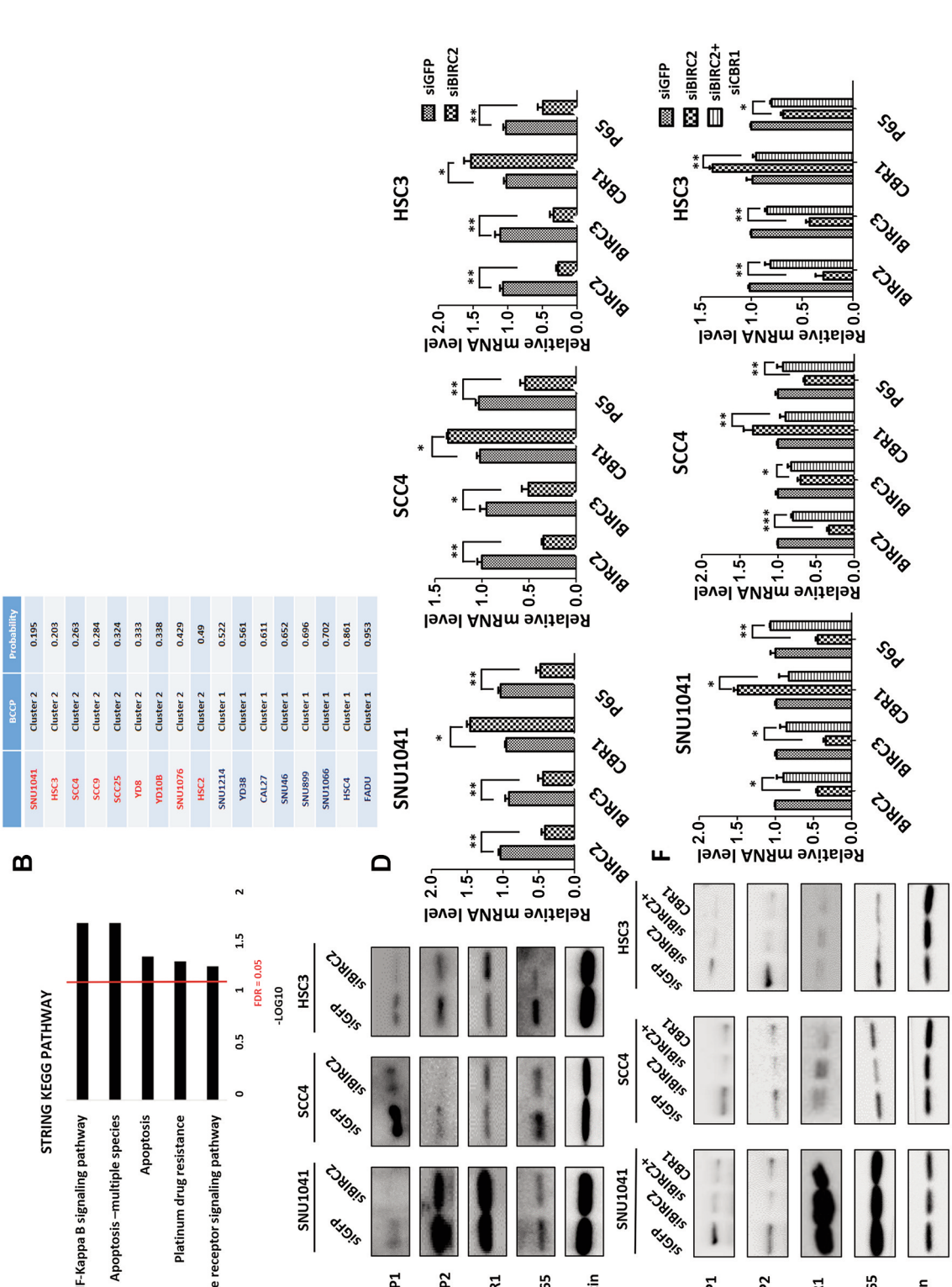

Figure 4. *Level of BIRC2 regulates CIAP2, CBR1, and P65 expression in HNSCC cancer. (A). Association of BIRC2-BIRC3 gene signature with NF-Kapp B signaling pathway. (B) The validation of BIRC2-BIRC3 gene signature with CCLE cell lines data. (C, D) SNU1041, SCC4 and HSC3 cells were transfected with siRNA targeting GFP or BIRC2. (C) The protein levels of CIAP1, CIAP2, CBR1, and P65 were determined by western blot analysis. (D) mRNA expressions of BIRC2, BIRC3, CBR1, and P65 were analyzed by qRT-PCR. (E, F) SNU1041, SCC4 and HSC3 cells were transfected with siRNA targeting CBR1 which is co-transfected with BIRC2. (E) The protein levels of CIAP1, CIAP2, CBR1, and P65 were determined by western blot analysis. (F) mRNA expressions of BIRC2, BIRC3, CBR1 and P65 were analyzed by qRT-PCR. β-actin was used as loading control. qRT-PCR experiments were performed in triplicate. *p<0.05 was established via a two-tailed independent t-test.*

Table IV. *Genes associated with BIRC3*.

TCGA RNA sequencing gene symbol	Correlation coefficient with copy number of BIRC3	*p*-Value of correlation with copy number of BIRC3	Correlation coefficient with gene expression of BIRC3	*p*-Value of correlation with gene expression of BIRC3
ABCD2	–0.25	4.96E-09	0.31	6.21E-13
ANKRD32	–0.26	1.82E-09	0.29	4.71E-11
ARHGAP26	–0.26	1.25E-09	0.46	3.51E-28
BCL2	–0.26	2.77E-09	0.37	6.18E-18
BIRC2	0.84	4.00E-135	0.47	3.46E-29
BIRC3	0.28	9.12E-11	1	0
C11orf70	0.42	1.61E-23	0.31	8.93E-13
CBX7	–0.28	1.03E-10	0.3	2.28E-12
CHPF	0.25	8.31E-09	–0.29	2.18E-11
CYP4X1	–0.25	7.16E-09	0.37	5.32E-18
ENDOD1	0.25	4.96E-09	–0.32	2.03E-13
FCHSD2	0.25	9.29E-09	0.34	2.43E-15
ISOC1	–0.25	6.88E-09	0.27	9.36E-10
KIAA1377	0.45	1.25E-26	0.37	2.03E-18
MAP3K14	–0.26	1.29E-09	0.4	4.07E-21
MGAT3	–0.25	8.54E-09	0.38	2.80E-19
NUTF2	0.27	9.62E-10	–0.27	5.55E-10
RELT	0.29	1.27E-11	0.27	4.87E-10
RHOD	0.25	5.38E-09	–0.26	2.21E-09
SLC7A5	0.25	8.09E-09	–0.29	2.11E-11
THEMIS	–0.26	4.06E-09	0.31	5.73E-13
TMEM123	0.7	1.73E-76	0.39	1.07E-19
UBD	–0.26	3.17E-09	0.48	2.51E-30
YAP1	0.78	1.80E-106	0.26	3.28E-09
ZMAT1	–0.27	9.83E-10	0.31	8.97E-13

Table V. *Univariate and multivariate Cox proportional hazard regression analysis of overall survival in the TCGA, Leipzig and KHU cohort (n=905)*.

	Univariate		Multivariate	
Variables	HR (95% CI)	*p*-Value	HR (95% CI)	*p*-Value
BIRC2-3 gene signature (Cluster2)	1.40 (1.11-1.78)	0.00474	1.29 (0.98-1.70)	0.0424
Sex (Male)	0.78 (0.59-1.01)	0.0608	0.92 (0.66-1.27)	0.6002
Age (>60 y)	1.31 (1.03-1.66)	0.0231	1.23 (0.94-1.61)	0.1289
Smoking (Yes)	1.02 (0.76-.1.36)	0.89	0.88 (0.63-1.24)	0.4781
Alcohol (Yes)	0.89 (0.68-1.16)	0.397	1.11 (0.80-1.54)	0.5374
Anatomic site (Oropharynx)	0.52 (0.31-0.88)	0.0158	1.28 (0.89-1.84)	0.1776
HPV status (HPV-positive)	0.42 (0.28-0.62)	2.86e-05	0.60 (0.37-0.98)	0.0509
Primary tumor (T3,4)	2.09 (0.48-1.60)	9.5e-08	2.50 (1.69-3.70)	5.18e-06
Regional lymph node (N+)	1.90 (1.47-2.44)	7.92e-07	1.77 (1.35-2.33)	3.04e-05
Stage (Stage III & IV)	1.27 (0.94-1.72)	0.112	0.78 (0.49-1.84)	0.2959

HR: Hazard ratio; CI: confidence interval.

Discussion

The present study used genomic copy number as well as mRNA expression data of BIRC2 and BIRC3 from the TCGA database to identify the most intriguing gene signature associated with clinical outcomes (BIRC2-BIRC3 gene signature). Two distinct clusters that were significantly associated with the prognosis of patients with HNSCC were identified, wherein Cluster 2 had a lower survival rate than Cluster 1. Furthermore, it was revealed that there was no statistically significant survival difference in patients with early tumor stage, while a statistically significant survival

difference was observed for patients with an advanced tumor stage. Finally, a functional study of the BIRC2-BIRC3 gene signature provided clues for the elucidation of potential therapeutic target genes.

The BIRC2 and BIRC3 genes that constitute this signature are intriguing from an oncological perspective. Since BIRC2 and BIRC3 are paralogous genes on chromosome 11q.22, copy number loss and somatic mutations have been frequently detected synchronously (12). Such genetic alterations contribute to carcinogenesis by activating oncogenic signaling pathways (13, 14). Moreover, BIRC2 and BIRC3 are known to be involved in poor prognosis in HNSCC and other cancers by modulating cell apoptosis, proliferation and invasion (14-17). BIRC3 mutations are related to tumor progression and treatment resistance (18). BIRC2 and BIRC3 has been discovered to be overexpressed in a wide variety of cancers through gene amplification (8, 19, 20). Overexpression of BIRC2 or BIRC3 has been reported to be involved in the poor prognosis of patients with glioblastoma, cervical cancer, and oral squamous cell carcinoma (OSCC) (21-24). Furthermore, BIRC2 and BIRC3 are widely expressed in a variety of cancer tissues, including pancreatic and breast cancers (25, 26). Previous studies have reported that BIRC2 and BIRC3 are overexpressed in a variety of noninvasive early stages of pancreatic cancer. The early events of BIRC2 and BIRC3 overexpression accelerated carcinogenesis and were maintained during tumor progression (27). In contrast, some studies have identified that BIRC2 mRNA expression is increased in tumor stages III or IV (28), and breast cancer patients with metastases had a correlation with BIRC2 mRNA expression. In this study, the BIRC2-BIRC3 gene signature was significantly associated with prognosis in advanced tumor stages. Thus, our novel gene signature can stratify patients with HNSCC into two distinct clusters in the advanced stages of the disease.

In demonstrating the association of the BIRC2-BIRC3 gene signature with the functional study, it was found that our robust gene signature was most relevant to NF-κB signaling. Moreover, copy number loss of BIRC2 and BIRC3 is involved in the activation of NF-κB signaling (8). NF-κB is one of the most important transcription factors linking the development and progression of many cancers, and its activation triggers various target genes, such as pro-proliferative and anti-apoptotic genes (29-32). NF-κB is a Rel family comprising five members: Rel-A (p65), Rel-B, Rel (c-Rel), NF-κB1 (p50/p105), and NF-κB2 (p52/p100) in mammals (33). NF-κB signaling crosstalk is involved in several signaling pathways including P53, Notch, Wnt –β-catenin, and NRF2 (33). These pleiotropic transcription factors influence oncogenesis and the prognosis of patients in various cancers (34-36).

Our previous studies demonstrated that CBR1 expression is critical to HNSCC patient survival by regulating the oxidative stress response (37). As an important factor involved in regulating oxidative stress and inflammation, CBR1 affects tumor progression, growth, as well as proliferation in several cancers, including ovarian cancer, endometrial cancer, and OSCC (38-40). In addition, suppression of CBR1 expression stimulates the epithelial mesenchymal transition (EMT) of cancer cells, with the induction of Wnt/β-catenin activation in HNSCC. CBR1 is also known to be involved in malignant behavior through the suppression of NF-κB signaling, which participates in EMT regulation (41). The present study explored the pathways associated with BIRC2, CBR1, and NF-κB. It was consequently hypothesized that BIRC2 is involved in the regulation of NF-κB *via* CBR1 expression. Our results suggest that the inhibition of BIRC2 increased CBR1 expression and decreased P65, a member of the NF-κB Rel family. In addition, inhibition of CBR1 led to the upregulation of P65, consistent with previous study results. This result indicated that CBR1 modulates P65 expression, as a downstream molecule of BIRC2.

Conclusion

In conclusion, we developed BIRC2-BIRC3 gene signature being able to predict the prognosis of HNSCC. It was validated in other independent cohorts. BIRC2-BIRC3 gene signature offers insight into the biological mechanisms of the BIRC2 and BIRC3 genes.

Conflicts of Interest

The Authors declare no potential conflicts of interest with respect to the research, authorship, and publication.

Authors' Contributions

Min Kyeong Lee and Young-Gyu Eun conceived of the presented idea, Joo Kyung Noh, Seon Rang Woo developed the theory and performed the computations. Moonkyoo Kong verified the analytical methods. Young Chan Lee, Jung Woo Lee, Seong-Gyu Ko contributed to the final version of the manuscript. Young-Gyu Eun supervised the project.

Acknowledgements

This work was supported by the National Research Foundation of Korea (NRF) grant funded by the Korea Government (MSIT) (No. 2020R1A5A2019413) and by a grant of the Korea Health Technology R&D Project through the Korea Health Industry Development Institute (KHIDI), funded by the Ministry of Health & Welfare, Republic of Korea (Grant No.: HI20C1205).

References

1 Vokes EE, Weichselbaum RR, Lippman SM and Hong WK: Head and neck cancer. N Engl J Med *328(3)*: 184-194, 1993. PMID: 8417385. DOI: 10.1056/NEJM199301213280306

2 Dhull AK, Atri R, Dhankhar R, Chauhan AK and Kaushal V: Major risk factors in head and neck cancer: a retrospective analysis of 12-year experiences. World J Oncol *9(3)*: 80-84, 2018. PMID: 29988794. DOI: 10.14740/wjon1104w

3 Ferlay J, Soerjomataram I, Dikshit R, Eser S, Mathers C, Rebelo M, Parkin DM, Forman D and Bray F: Cancer incidence and mortality worldwide: sources, methods and major patterns in GLOBOCAN 2012. Int J Cancer *136(5)*: E359-E386, 2015. PMID: 25220842. DOI: 10.1002/ijc.29210

4 Gupta S, Kong W, Peng Y, Miao Q and Mackillop WJ: Temporal trends in the incidence and survival of cancers of the upper aerodigestive tract in Ontario and the United States. Int J Cancer *125(9)*: 2159-2165, 2009. PMID: 19569190. DOI: 10.1002/ijc.24533

5 Chang JH, Wu CC, Yuan KS, Wu ATH and Wu SY: Locoregionally recurrent head and neck squamous cell carcinoma: incidence, survival, prognostic factors, and treatment outcomes. Oncotarget *8(33)*: 55600-55612, 2017. PMID: 28903447. DOI: 10.18632/oncotarget.16340

6 Estornes Y and Bertrand MJ: IAPs, regulators of innate immunity and inflammation. Semin Cell Dev Biol *39*: 106-114, 2015. PMID: 24718315. DOI: 10.1016/j.semcdb.2014.03.035

7 Evan GI and Vousden KH: Proliferation, cell cycle and apoptosis in cancer. Nature *411(6835)*: 342-348, 2001. PMID: 11357141. DOI: 10.1038/35077213

8 Asslaber D, Wacht N, Leisch M, Qi Y, Maeding N, Hufnagl C, Jansko B, Zaborsky N, Villunger A, Hartmann TN, Greil R and Egle A: BIRC3 expression predicts CLL progression and defines treatment sensitivity *via* enhanced NF-κB nuclear translocation. Clin Cancer Res *25(6)*: 1901-1912, 2019. PMID: 30487125. DOI: 10.1158/1078-0432.CCR-18-1548

9 Yamato A, Soda M, Ueno T, Kojima S, Sonehara K, Kawazu M, Sai E, Yamashita Y, Nagase T and Mano H: Oncogenic activity of BIRC2 and BIRC3 mutants independent of nuclear factor-κB-activating potential. Cancer Sci *106(9)*: 1137-1142, 2015. PMID: 26094954. DOI: 10.1111/cas.12726

10 Eisen MB, Spellman PT, Brown PO and Botstein D: Cluster analysis and display of genome-wide expression patterns. Proc Natl Acad Sci U.S.A. *95(25)*: 14863-14868, 1998. PMID: 9843981. DOI: 10.1073/pnas.95.25.14863

11 Helman P, Veroff R, Atlas SR and Willman C: A Bayesian network classification methodology for gene expression data. J Comput Biol *11(4)*: 581-615, 2004. PMID: 15579233. DOI: 10.1089/cmb.2004.11.581

12 Tanimoto T, Tsuda H, Imazeki N, Ohno Y, Imoto I, Inazawa J and Matsubara O: Nuclear expression of cIAP-1, an apoptosis inhibiting protein, predicts lymph node metastasis and poor patient prognosis in head and neck squamous cell carcinomas. Cancer Lett *224(1)*: 141-151, 2005. PMID: 15911110. DOI: 10.1016/j.canlet.2004.11.049

13 Bhosale PG, Pandey M, Cristea S, Shah M, Patil A, Beerenwinkel N, Schäffer AA and Mahimkar MB: Recurring amplification at 11q22.1-q22.2 locus plays an important role in lymph node metastasis and radioresistance in OSCC. Sci Rep *7(1)*: 16051, 2017. PMID: 29167558. DOI: 10.1038/s41598-017-16247-y

14 Macaluso M, Paggi MG and Giordano A: Genetic and epigenetic alterations as hallmarks of the intricate road to cancer. Oncogene *22(42)*: 6472-6478, 2003. PMID: 14528270. DOI: 10.1038/sj.onc.1206955

15 Bertrand MJ, Milutinovic S, Dickson KM, Ho WC, Boudreault A, Durkin J, Gillard JW, Jaquith JB, Morris SJ and Barker PA: cIAP1 and cIAP2 facilitate cancer cell survival by functioning as E3 ligases that promote RIP1 ubiquitination. Mol Cell *30(6)*: 689-700, 2008. PMID: 18570872. DOI: 10.1016/j.molcel.2008.05.014

16 Lin RJ, Lubpairee T, Liu KY, Anderson DW, Durham S and Poh CF: Cyclin D1 overexpression is associated with poor prognosis in oropharyngeal cancer. J Otolaryngol Head Neck Surg *42*: 23, 2013. PMID: 23672832. DOI: 10.1186/1916-0216-42-23

17 Yang L, Kumar B, Shen C, Zhao S, Blakaj D, Li T, Romito M, Teknos TN and Williams TM: LCL161, a SMAC-mimetic, preferentially radiosensitizes human papillomavirus-negative head and neck squamous cell carcinoma. Mol Cancer Ther *18(6)*: 1025-1035, 2019. PMID: 31015310. DOI: 10.1158/1535-7163.MCT-18-1157

18 Jiang X, Li C, Lin B, Hong H, Jiang L, Zhu S, Wang X, Tang N, Li X, She F and Chen Y: cIAP2 promotes gallbladder cancer invasion and lymphangiogenesis by activating the NF-κB pathway. Cancer Sci *108(6)*: 1144-1156, 2017. PMID: 28295868. DOI: 10.1111/cas.13236

19 Gressot LV, Doucette T, Yang Y, Fuller GN, Manyam G, Rao A, Latha K and Rao G: Analysis of the inhibitors of apoptosis identifies BIRC3 as a facilitator of malignant progression in glioma. Oncotarget *8(8)*: 12695-12704, 2017. PMID: 27074575. DOI: 10.18632/oncotarget.8657

20 Falkenhorst J, Grunewald S, Mühlenberg T, Marino-Enriquez A, Reis AC, Corless C, Heinrich M, Treckmann J, Podleska LE, Schuler M, Fletcher JA and Bauer S: Inhibitor of Apoptosis Proteins (IAPs) are commonly dysregulated in GIST and can be pharmacologically targeted to enhance the pro-apoptotic activity of imatinib. Oncotarget *7(27)*: 41390-41403, 2016. PMID: 27167336. DOI: 10.18632/oncotarget.9159

21 Che X, Yang D, Zong H, Wang J, Li X, Chen F, Chen X and Song X: Nuclear cIAP1 overexpression is a tumor stage- and grade-independent predictor of poor prognosis in human bladder cancer patients. Urol Oncol *30(4)*: 450-456, 2012. PMID: 21795072. DOI: 10.1016/j.urolonc.2010.12.016

22 Nagata M, Nakayama H, Tanaka T, Yoshida R, Yoshitake Y, Fukuma D, Kawahara K, Nakagawa Y, Ota K, Hiraki A and Shinohara M: Overexpression of cIAP2 contributes to 5-FU resistance and a poor prognosis in oral squamous cell carcinoma. Br J Cancer *105(9)*: 1322-1330, 2011. PMID: 21952624. DOI: 10.1038/bjc.2011.387

23 Bai L, Smith DC and Wang S: Small-molecule SMAC mimetics as new cancer therapeutics. Pharmacol Ther *144(1)*: 82-95, 2014. PMID: 24841289. DOI: 10.1016/j.pharmthera.2014.05.007

24 Wang D, Berglund AE, Kenchappa RS, MacAulay RJ, Mulé JJ and Etame AB: BIRC3 is a biomarker of mesenchymal habitat of glioblastoma, and a mediator of survival adaptation in hypoxia-driven glioblastoma habitats. Sci Rep *7(1)*: 9350, 2017. PMID: 28839258. DOI: 10.1038/s41598-017-09503-8

25 Imoto I, Yang ZQ, Pimkhaokham A, Tsuda H, Shimada Y, Imamura M, Ohki M and Inazawa J: Identification of cIAP1 as a candidate target gene within an amplicon at 11q22 in esophageal squamous cell carcinomas. Cancer Res *61(18)*: 6629-6634, 2001. PMID: 11559525.

26 Uhlen M, Oksvold P, Fagerberg L, Lundberg E, Jonasson K, Forsberg M, Zwahlen M, Kampf C, Wester K, Hober S, Wernerus H, Björling L and Ponten F: Towards a knowledge-

based Human Protein Atlas. Nat Biotechnol *28(12)*: 1248-1250, 2010. PMID: 21139605. DOI: 10.1038/nbt1210-1248

27 Esposito I, Kleeff J, Abiatari I, Shi X, Giese N, Bergmann F, Roth W, Friess H and Schirmacher P: Overexpression of cellular inhibitor of apoptosis protein 2 is an early event in the progression of pancreatic cancer. J Clin Pathol *60(8)*: 885-895, 2007. PMID: 16775116. DOI: 10.1136/jcp.2006.038257

28 Kempkensteffen C, Jäger T, Bub J, Weikert S, Hinz S, Christoph F, Krause H, Schostak M, Miller K and Schrader M: The equilibrium of XIAP and Smac/DIABLO expression is gradually deranged during the development and progression of testicular germ cell tumours. Int J Androl *30(5)*: 476-483, 2007. PMID: 17298543. DOI: 10.1111/j.1365-2605.2006.00742.x

29 Hayden MS and Ghosh S: Signaling to NF-kappaB. Genes Dev *18(18)*: 2195-2224, 2004. PMID: 15371334. DOI: 10.1101/gad.1228704

30 Luo JL, Kamata H and Karin M: IKK/NF-kappaB signaling: balancing life and death—a new approach to cancer therapy. J Clin Invest *115(10)*: 2625-2632, 2005. PMID: 16200195. DOI: 10.1172/JCI26322

31 Baldwin AS: Control of oncogenesis and cancer therapy resistance by the transcription factor NF-kappaB. J Clin Invest *107(3)*: 241-246, 2001. PMID: 11160144. DOI: 10.1172/JCI11991

32 Karin M and Ben-Neriah Y: Phosphorylation meets ubiquitination: the control of NF-[kappa]B activity. Annu Rev Immunol *18*: 621-663, 2000. PMID: 10837071. DOI: 10.1146/annurev.immunol.18.1.621

33 Webster GA and Perkins ND: Transcriptional cross talk between NF-kappaB and p53. Mol Cell Biol *19(5)*: 3485-3495, 1999. PMID: 10207072. DOI: 10.1128/MCB.19.5.3485

34 Ma B and Hottiger MO: Crosstalk between Wnt/β-Catenin and NF-κB signaling pathway during inflammation. Front Immunol *7*: 378, 2016. PMID: 27713747. DOI: 10.3389/fimmu.2016.00378

35 Mishra AK, Sharma V, Mutsuddi M and Mukherjee A: Signaling cross-talk during development: Context-specific networking of Notch, NF-κB and JNK signaling pathways in Drosophila. Cell Signal *82*: 109937, 2021. PMID: 33529757. DOI: 10.1016/j.cellsig.2021.109937

36 Simplicio-Revoredo CM, de Oliveira Pereira R, de Almeida Melo M, Lopes-Costa PV, de Tarso Moura-Borges P, Sousa EB, Neto FM, Campelo V, Soares-Lopes IMR, da Conceição Barros-Oliveira M, Tavares CB, Dos Santos AR, de Araújo CGB, Coelho EG, Campos-Verdes LC, do Nascimento-Holanda AO, Viana JL, Bezerra-Chaves MLM, de Vasconcelos-Valença RJ, Dos Santos LG, Soares-Lopes LR, Pinho-Sobral AL, Gebrim LH and da Silva BB: Expression of Nrf2 and NF-κB transcription factors in breast cancer and breast fibroadenoma: Insights for a new therapeutic approach. Oncotarget *11(18)*: 1629-1636, 2020. PMID: 32405338. DOI: 10.18632/oncotarget.27574

37 Yun M, Choi AJ, Lee YC, Kong M, Sung JY, Kim SS and Eun YG: Carbonyl reductase 1 is a new target to improve the effect of radiotherapy on head and neck squamous cell carcinoma. J Exp Clin Cancer Res *37(1)*: 264, 2018. PMID: 30376862. DOI: 10.1186/s13046-018-0942-9

38 Osawa Y, Yokoyama Y, Shigeto T, Futagami M and Mizunuma H: Decreased expression of carbonyl reductase 1 promotes ovarian cancer growth and proliferation. Int J Oncol *46(3)*: 1252-1258, 2015. PMID: 25572536. DOI: 10.3892/ijo.2014.2810

39 Murakami A, Yakabe K, Yoshidomi K, Sueoka K, Nawata S, Yokoyama Y, Tsuchida S, Al-Mulla F and Sugino N: Decreased carbonyl reductase 1 expression promotes malignant behaviours by induction of epithelial mesenchymal transition and its clinical significance. Cancer Lett *323(1)*: 69-76, 2012. PMID: 22542806. DOI: 10.1016/j.canlet.2012.03.035

40 Kim YN, Kim DW, Jo HS, Shin MJ, Ahn EH, Ryu EJ, Yong JI, Cha HJ, Kim SJ, Yeo HJ, Youn JK, Hwang JH, Jeong JH, Kim DS, Cho SW, Park J, Eum WS and Choi SY: Tat-CBR1 inhibits inflammatory responses through the suppressions of NF-κB and MAPK activation in macrophages and TPA-induced ear edema in mice. Toxicol Appl Pharmacol *286(2)*: 124-134, 2015. PMID: 25818598. DOI: 10.1016/j.taap.2015.03.020

41 Yun M, Choi AJ, Woo SR, Noh JK, Sung JY, Lee JW and Eun YG: Inhibition of carbonyl reductase 1 enhances metastasis of head and neck squamous cell carcinoma through β-catenin-mediated epithelial-mesenchymal transition. J Cancer *11(3)*: 533-541, 2020. PMID: 31942176. DOI: 10.7150/jca.34303

Received March 22, 2022
Revised June 23, 2022
Accepted June 29, 2022